DOI:
10.1016/j.microrel.2016.06.007

Document Version
Peer reviewed version

Microstructural evolution of sintered silver at elevated temperatures

Seyed Amir Paknejad*, Ali Mansourian, Julian Greenberg, Khalid Khtatba, Linde Van Parijs, Samjid H. Mannan

King's College London

Physics Department, Strand, London, WC2R 2LS, UK

Tel: 44 (0) 790 272 2739 Fax: 44 (0) 207 848 2420 Email: sa.paknejad@kcl.ac.uk

*Corresponding author

Abstract

Reduction in the sintering temperature of metal powders by lowering particle size into the nanoparticle range has resulted in a new class of porous sintered joining materials. Especially promising are sintered silver based materials which can be used to form bonds between wide-bandgap semiconductor die and circuit boards for use in high temperature applications. This work shows that for these materials the exterior sintered silver surface oxidizes preventing surface morphology changes, while the interior pore surfaces of the porous silver remain largely oxide-free. These pore surfaces facilitate fast atomic movement resulting in grain growth and changes in the internal microstructure. Morphology changes in the temperature range 200-400 °C are presented both as statistical averages of grain size and, uniquely in this type of study, by tracking individual pores and grains. It is shown that the internal structure will undergo changes during high temperature storage in contrast to the stable outer surface. A new technique, utilizing the electromigration effect to check the relative surface mobility of atoms in the interior pores and exterior surfaces was used to support the conclusions deduced from thermal ageing

experiments. Finally, we speculate that the stability of the exterior surface could be reproduced in the interior if the chemistry of the paste was altered to allow formation of a passivating layer on the interior pores during the final stages of the sintering process, resulting in formation of a stable die attach material for applications of up to 400 °C, for which there is an urgent need.

Keywords: Grain Growth, Sintering, Porous Materials, Aging, Silver Nanoparticle Paste, Bonding.

1. Introduction

The operating temperature of electronic materials in hybrid automotive, aerospace, space exploration, and deep oil and gas exploration can reach 300 °C and beyond [1]. Current high temperature die attach materials such as high temperature solders or Solid Liquid Inter-Diffusion (SLID) bonding materials suffer from high homologous temperatures and Pb content in case of high temperature solders or rapid reduction in mechanical strength by increase in temperature in case of SLID systems [2]. Therefore, there is a requirement for new joining materials that can be processed at low temperatures but that retains joint strength at high temperatures.

One of the potential solutions involves utilization of the unique properties of nanoparticles. By reduction in particle size, the ratio between surface area and volume increases, contributing to a rise in surface energy and a melting point that is considerably lower than that of the bulk material [3]. For example, in the case of silver the melting point of bulk silver is 961 °C, while melting point of 2.4 nm silver particles is 350 °C [4]. This feature of nanoparticles has been researched in the past decade in order to decouple the processing temperature from operating temperature of high-temperature electronic packaging materials, with silver receiving special interest because of its desirable mechanical, electrical and thermal properties [4-9] as well as the noble metal nature of silver that prevents excessive oxide formation. In this case, the attachment or interconnects can be formed at considerably lower temperatures than the melting point of the bulk material which determines the ultimate operating temperature. The high surface energy available and noble metal surface of silver also allows sintering to take place without

pressure being placed on the die; an added benefit for manufacturers, but one which leads to the final sintered structure containing 20-30% of pores.

Although many studies have been performed on the sintering behaviour of nanoparticles [10, 11], and also the mechanical properties of their sintered structures [8,9,12,13], there exists few detailed studies on the high temperature behaviour and stability of sintered silver at temperatures above 300 °C as a high temperature die attach (excepting [14-15]), while previous studies below 300 °C concentrate on bulk mechanical properties and statistical averages of microstructural properties [8,9,16-20]. In the present work, we determine the nature and speed of microstructural changes in sintered silver throughout the 200-400 °C temperature range and investigate the atomic migration mechanisms that lead to these changes. Tracking of changes in individual grains and pores is found to be complicated by the fact that any exposure of the internal pore surfaces to air leads to rapid oxidation and freezing of the microstructure in its original state, similarly to the original exterior surface of the material. Therefore, we have utilized optical microscopy and a glass substrate to prevent the internal pore surfaces from oxidizing while enabling in-situ observations to take place. These microstructural changes would in most cases lead to unreliability and weakening strength [9, 17-19] so that these studies are an innovative technique for understanding long term mechanical reliability and strength preservation of sintered silver for applications in the range 200-400 °C.

2. Experimental

In these studies, two commercially available silver nanoparticle pastes produced by NBE Tech under the names of NanoTach® X and NanoTach® N have been utilised.

NanoTach® N is recommended for small size die of 3×3 mm, while NanoTach® X is recommended for attachment of 10×10 mm die in a pressure-less sintering process. The composition of NanoTach® X is shown in Table 1 below. The assemblies, listed in Table 2, were all sintered using the recommended temperature profile from the paste manufacturer under zero applied pressure.

Table 1: NanoTach® X composition.

Components	Weight Percent
Silver	70-85
Silver Oxide	0-10
Cellulose	1-8
Alpha Terpineol	5-20
Menhaden Fish Oil	0-2
Isopropanol	<1
Ethanol	<1

In a previous study [19], samples were cross sectioned after sintering, and aged at 300 °C for 24, 100 and 500 h to track properties such as porosity and average pore size. In that study the evolution of individual pores and grains could not be tracked continuously. In the current experiments, in order to track changes occurring inside the sintered silver microstructure and investigate them continuously, samples were assembled by manual deposition of the NanoTach® X paste onto glass slides followed by placement of approximately 150 μm thick, 10×10 mm Menzel-Gläser cover-slips on top of the paste. To investigate the grain growth mechanisms of the sintered silver, these samples have been placed on a cartridge heater at 250, 300, 350 and 400 °C and the grain evolution has been observed in-situ for up to 7 h using an optical microscope (See Fig. 1), while one sample has been placed inside a furnace at 200 °C for 5 h. This experiment is referred to as sample set 1.

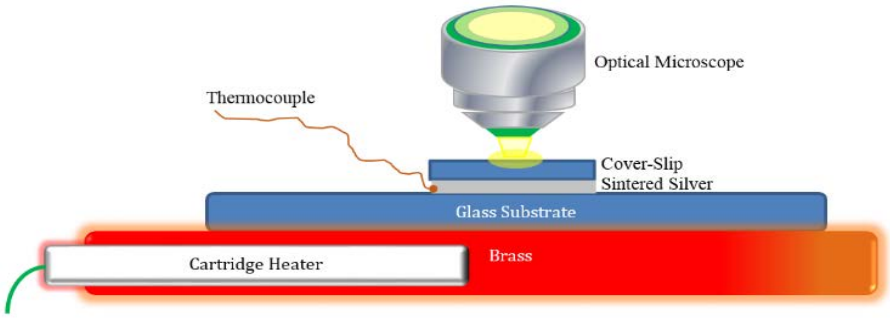

Fig. 1. Schematic representation of the experimental setup for in-situ observation of the changes to the grain structure of sintered silver at high temperature. (Cartridge heater was inserted inside the brass)

Observation of high temperature behaviour of sintered silver structure through the cover-slip provides information on microstructural changes similar to those occurring inside non-sectioned samples which have not been exposed to air. The presence of the cover-slip planarizes the initial microstructure and may affect parameters such as local porosity. However, comparison with samples that have been aged at 300 °C and then cross-sectioned [19] show qualitatively similar results indicating that the same mechanisms are active. The optical images were then analysed using Image J 1.46r coupled with the image processing toolbox in Matlab with a methodology [21] that allowed the microstructural evolution of sintered silver at high temperatures to be studied statistically (e.g. average grain size). In this method the optical images of the sintered structures have been segmented using an Image J predesigned function to separate the grains and their sizes have been measured using Matlab to calculate the average grain sizes.

The second set of samples was prepared by deposition of the paste into wire shaped gaps with approximate dimensions of 1 mm by 1 mm cross-section and 3 mm length for the first sample and approximately 150 μm by 150 μm cross section and 4 mm length for the remaining samples of this set. The first sample was stored at 300 °C in air and the

remainder were stored at 300 and 400 °C inside a vacuum of 5 mPa and at 450 and 500 °C in air to study microstructural evolution of the free surfaces.

The third sample set consisted of a single sample selected for thermal ageing after being first cross sectioned and polished in an attempt to observe evolution of the interior of sintered silver continuously. After the sintering step using NanoTach® N followed by cross sectioning, the sample was mounted using a hot mounting resin (LevoFast) from Struers, which consisted of melamine with minerals and glass filler. The sample was mechanically polished using successively finer grades of silicon carbide cloth before final polishing with water based suspensions of 3 and 0.25 micron mono-crystalline diamonds. The hot mounting resin was selected to withstand high temperature storage. The assembly was stored at 300 °C in air in an oven for 1, 4, 5, and 20 h consecutively (30 h in total), and observed under a Scanning Electron Microscope (SEM) to track changes.

The fourth set of samples were prepared by sintering of the NanoTach® X paste inside glass sample holders, which were designed for surface cleaning of the samples by perchloric acid (effective for removing organic contamination on silver without causing damage from the utilised concentration [22, 23]) before high temperature storage. After manual deposition of paste into the holder and sintering, the samples were stored for 30 minutes inside an aqueous solution containing 20% concentration of perchloric acid and then stored in deionised water before placement into the furnace for high temperature storage at 300 °C inside ~40 mPa vacuum for 5 h.

The fifth set of samples were prepared using the NanoTach® X paste with the same dimensions as the third set for electromigration studies [24]. These samples were subjected to high current densities of 2.4×10^8 A/m^2 for periods ranging from 20-25 days

before cross sectioning in order to compare atomic migration patterns on the surface and interior of the porous material.

The free surfaces of the sintered silver were observed using a Hitachi S4000 SEM coupled with Electron Dispersive X-ray (EDX) for elemental analysis.

Table 2: Sample sets.

Sample set No.	Purpose of experiment	Paste type and surface dimensions
1	Observation of microstructure evolution on a surface not exposed to air using optical microscope.	NanoTach® X 10 × 10 mm × 100 μm
2	Observation of exterior surface evolution under different atmospheres using SEM.	NanoTach® X 150 × 150 μm × 4 mm and 1 × 1 × 3 mm
3	Observation of interior microstructure evolution after cross sectioning using SEM.	NanoTach® N 2.5 × 2.5 mm × 30 μm
4	Observation of exterior surface evolution after acid cleaning using SEM.	NanoTach® X $r = 2$ mm
5	Comparison of exterior and interior atomic migration patterns during electromigration using SEM.	NanoTach® X 175 × 175 × 812 μm

3. Results and Discussion

3.1. Observation of microstructural evolution in the absence of air.

Fig. 2 shows optical images from sample set 1 of three samples stored at constant temperatures of 250, 350 and 400 °C showing the continuous evolution of microstructure adjacent to the cover-slip. Fig. 3 is a more detailed examination of the 350 °C sample clearly showing coarsening of the microstructure. Using image processing software, the average grain sizes from the images were calculated and plotted in Fig. 4. For the 400 °C sample, the grain sizes go through three grain growth phases, each having a lower slope than the preceding grain growth phase as a result of increase in the initial grain sizes. The first

phase of grain growth is defined as the period between start of heating to the point where the grain growth rate has decreased to a constant, low value. The second growth phase starts when the grain growth rate increases again and ends where the growth rate stabilizes again at a low value. For the 350 °C sample, after the first growth phase the average grain size remains almost constant for about 3.5 hours before entering the second growth phase. This may be due to the fact that during this period reorientation of grains is required before further coalescence. The 250 and 300 °C samples showed that grain sizes reached a similar stable point after an initial grain growth phase. However, there may be further growth phases outside the timescale of the current experiments for those samples. In contrast, the faster diffusion mechanisms at 400 °C have caused the shortening of the grain growth phases such that a larger number of phases are observable within the timescale of the experiment. At the lowest experimental temperature of 200 °C storage of sintered silver for 5 h did not indicate any grain growth implying greater stability of sintered silver material for such operating temperatures. Average grain size as a function of temperature is plotted in Fig. 5 for different storage times.

Errors for the average grain sizes have been calculated by performing five separate calculations of average grain size on random areas of the 350 °C sample after 90 minutes storage, which would provide a roughly middle point example. The standard deviation of those measurements has been used as the error for the average grain size of that particular temperature and time. The errors for the remaining average grain sizes has the same ratio to their corresponding average grain size values of the ratio of the measured error to its original average grain size.

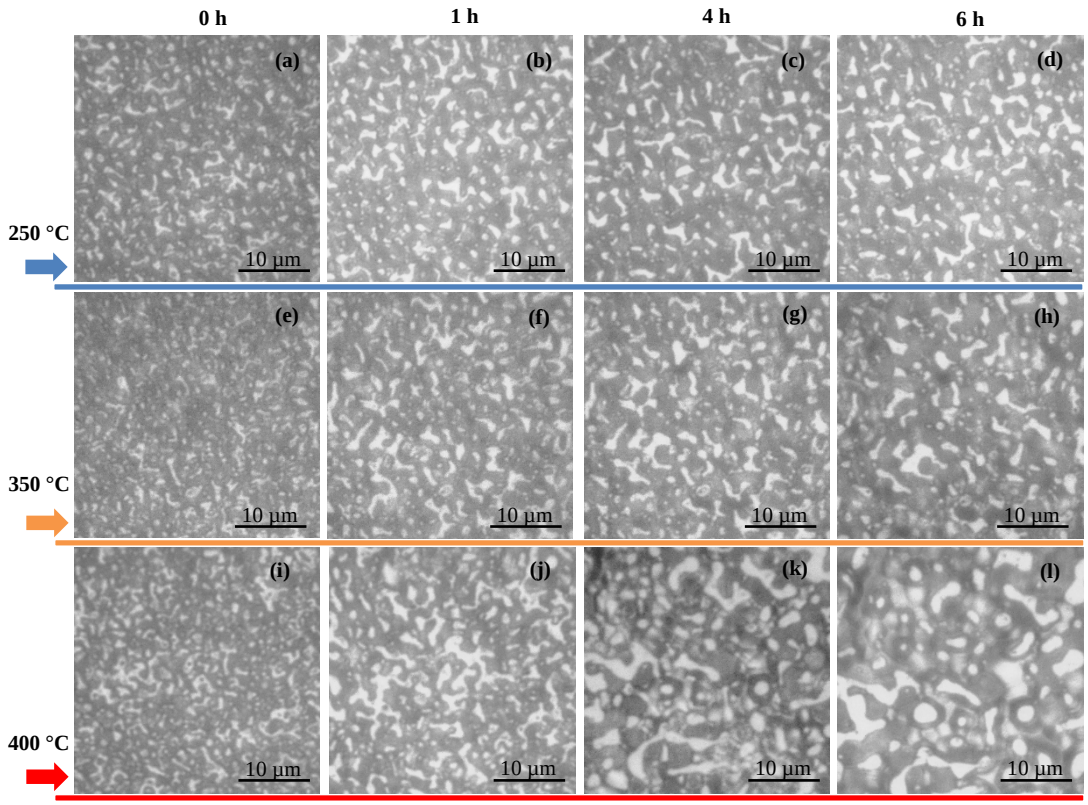

Fig. 2. Optical images of sintered silver under cover slip stored at high temperatures on top of a cartridge heater. (a-d) 250 °C storage. (e-h) 350 °C storage. (i-l) 400 °C storage.

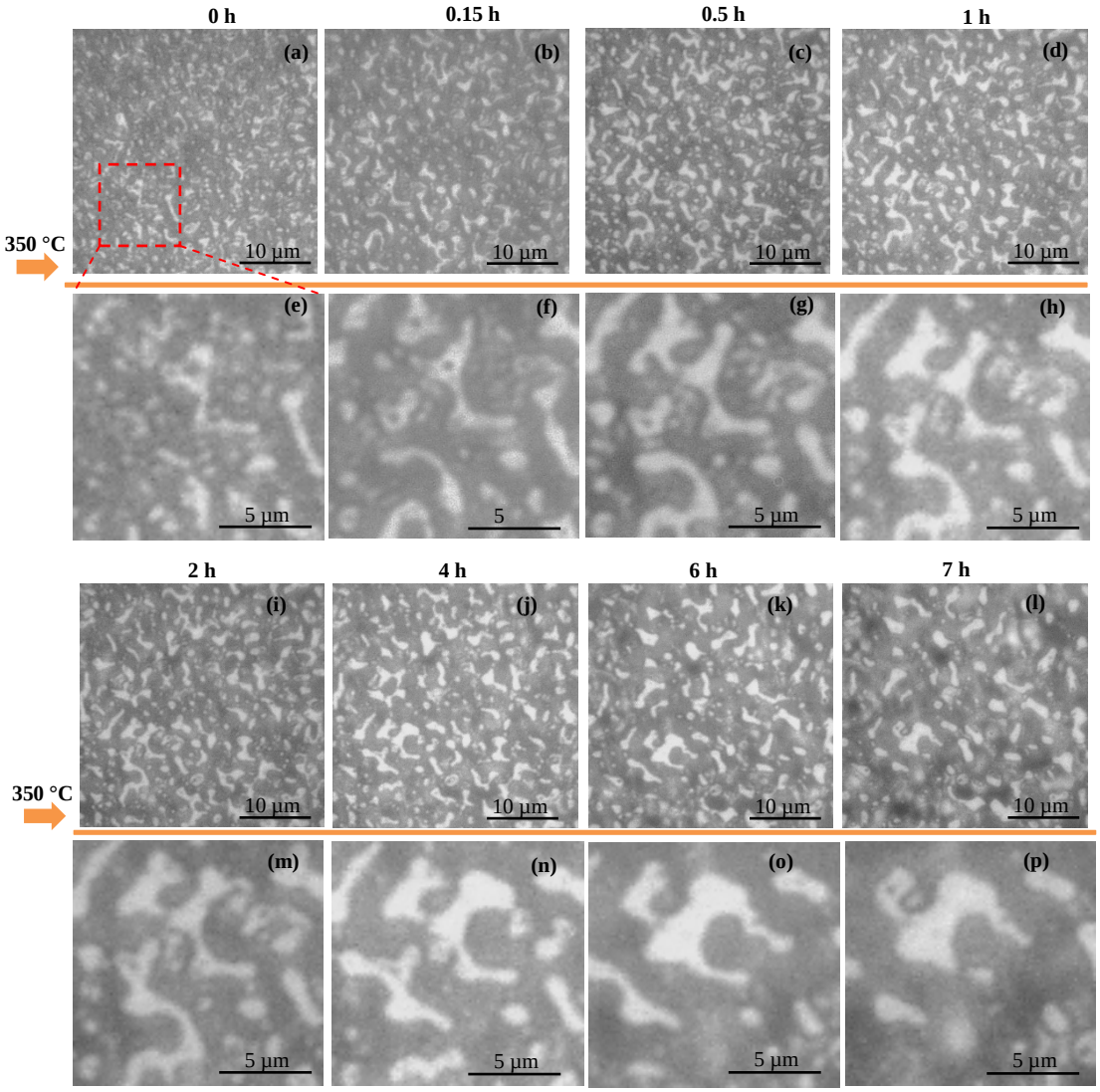

Fig. 3. Optical images showing continuous microstructural evolution of sintered silver under cover slip at 350 °C.

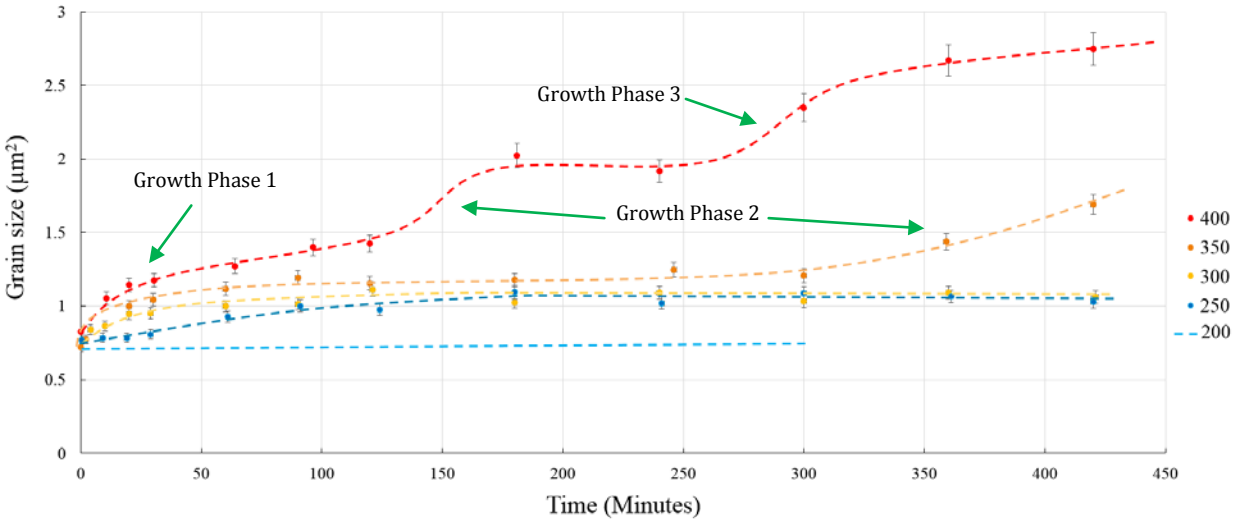

Fig. 4. Grain growth vs. time. (The curves are fitted manually for improved illustration)

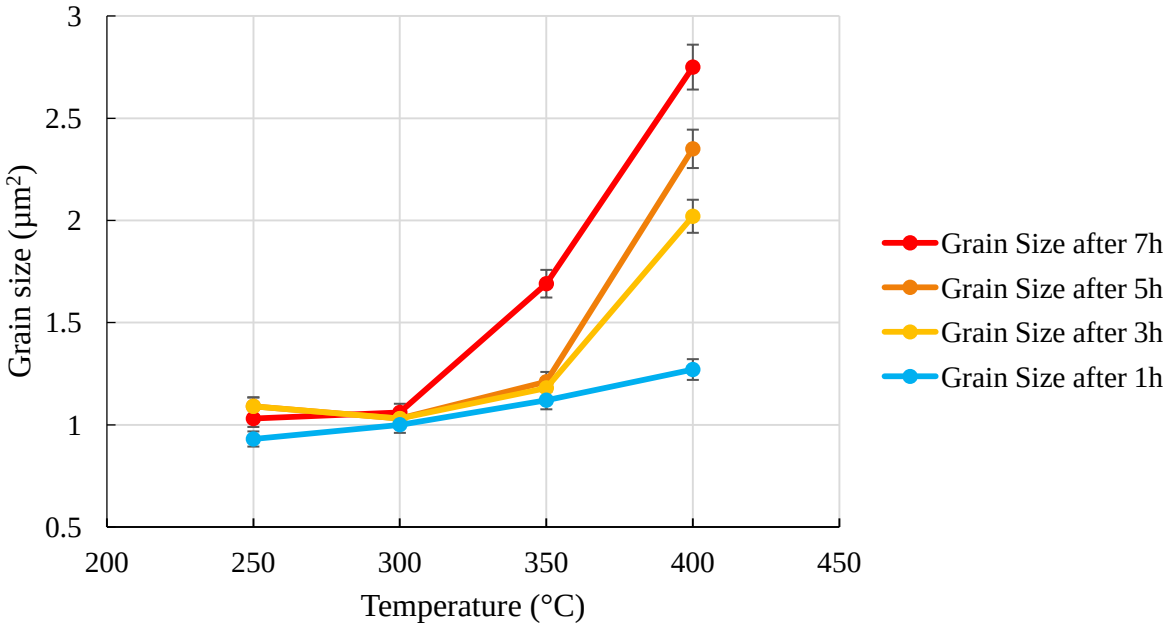

Fig. 5. Grain growth vs. temperature.

The general formula describing the rate of grain growth of the average grain size as a function of time can be written as [25]:

$$G^n - G_0^n = kt \quad (1)$$

where G is a parameter meauring linear grain size at time t and G_0 is the grain size at time zero, n is the grain growth exponent, and k is a grain growth constant, and has the proportionality relationship below [26]:

$$k \propto e^{-Q/RT} \tag{2}$$

where Q is the grain growth activation energy, R is the ideal gas constant and T is the temperature.

Dannenberg (2000) [26] estimated the value of n as 3 for grain growth of nanocrystaline silver and also for diffusion based grain growth, being applied here, it has been generally best fitted by $n = 3$ as well [25]. Therefore, for the intial grain growth phase of the samples G^3 has been ploted against t to find the slope of the grain growth, shown in Fig. 6. For the second phases which have been found for the 350 and 400 °C sample, this relationship has been plotted in Fig. 7.

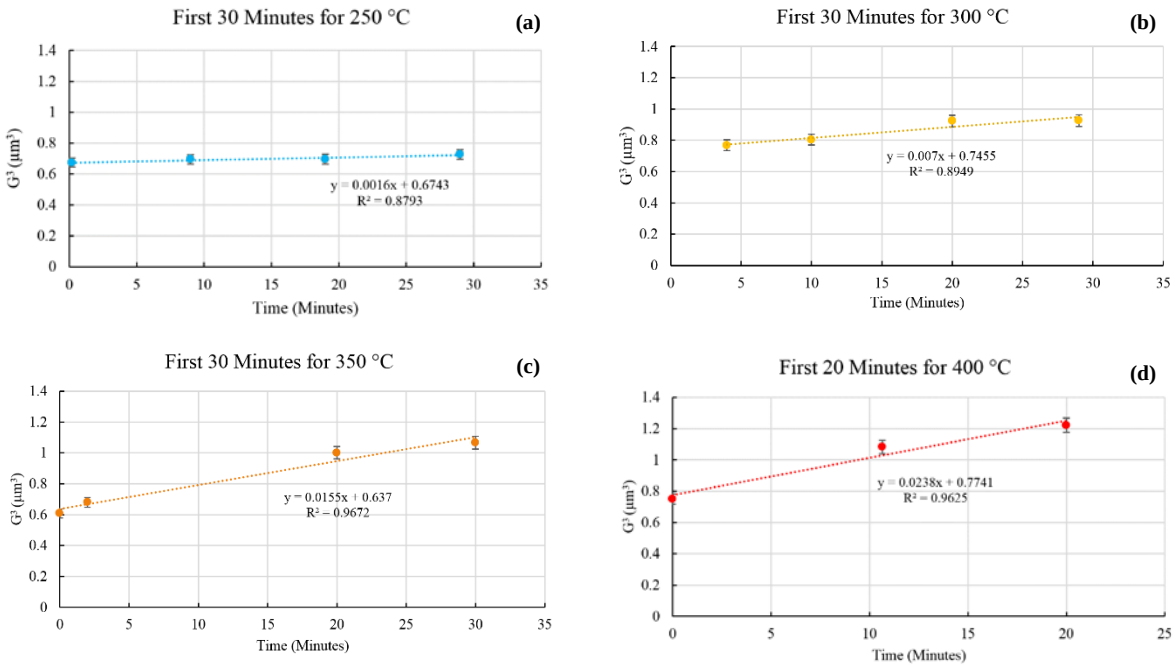

Fig. 6. Initial grain growth vs. time.

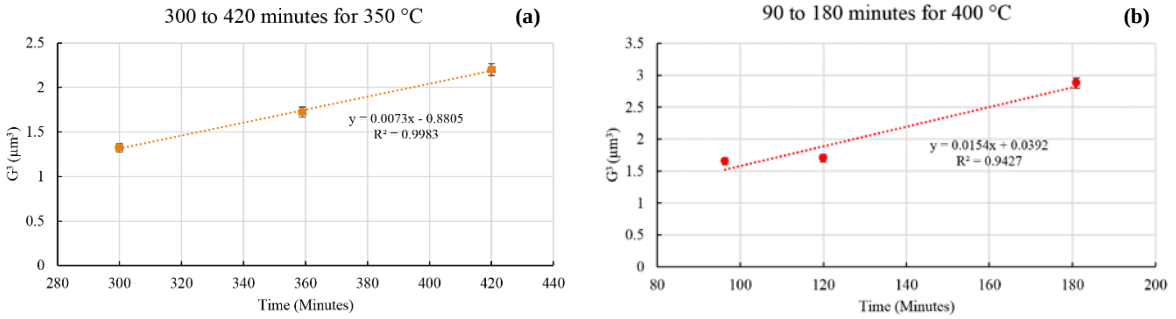

Fig. 7. Grain growth vs. time of the second grain growth phase.

By plotting the ln k against $1/T$, the activation energy of the grain growth can be calculated from the slopes for each of the grain growth phases from Eq. 2 (Fig. 8). As the second growth phase only occurred for the 350 °C and 400 °C samples, Fig. 8 (b) only contains two points. Therefore the activation energy calculated from the slope should be treated with caution.

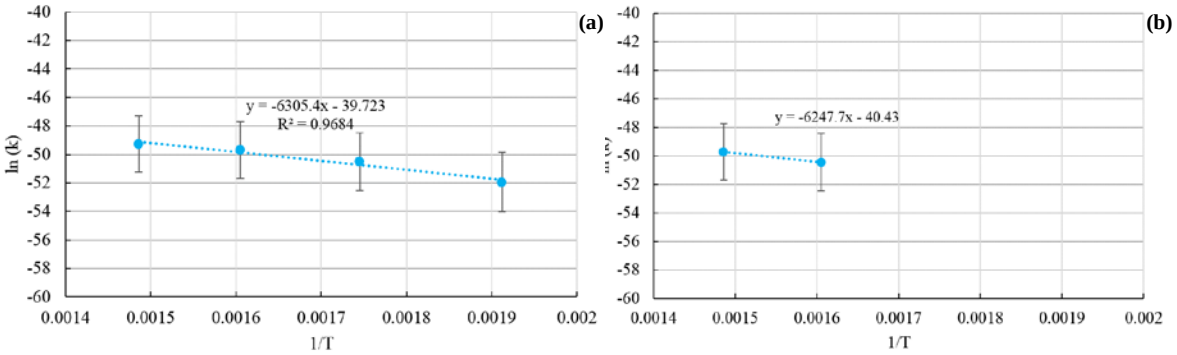

Fig. 8. ln(k) vs. reciprocal of temperature. (a) For the first grain growth phase. (b) For the second grain growth phase.

The grain growth activation energies calculated for the first and second phases are 53 ± 2 kJ/mol and 52 ± 2 kJ/mol respectively. These values are in accordance with the literature value of 53 kJ/mol [26].

The cited literature value of the activation energy for grain growth was calculated for nano sized silver grains, and the initial size of the second grain growth phases were about twice the initial sizes for the first phase, but all provide the same activation energy. Therefore, these results indicate that the activation energies of grain growth are independent of the initial sizes up to ~2 μm^2. Moreover, the similarity of the grain growth activation energy of the literature value, for which the grains were sputter-deposited, with the activation energy of the silver sintered under a cover-slip also confirms minimal contribution of the cover-slip to the diffusion mechanism of silver and its growth mechanisms.

While the rate of change of grain growth should be theoretically linearly dependent on surface diffusion and molar volume of the diffusing materials, on dimensional grounds we might expect the dependence of k on surface diffusitivity to vary as:

$$k = C\,\frac{D_S\,\gamma\,V_m}{R\,T} \qquad (3)$$

where D_S is the surface diffusion (measured values shown in Fig. 9), γ is the surface energy, (measured to be 1.14 J/m^2 [27]), V_m is the molar volume (1.03 × 10^{-5} m^3/mol), and C is a dimensionless constant (see e.g. [28] for a similar derivation). Fig. 9 shows the experimentally determined k value compared to the theoretical values computed from Eq. 3. The large discrepancy between the two shows that surface diffusion on a clean silver surface is not occuring and that a passivation layer on the interior pore surface also exists. The most likely explanation is that some organics from the silver paste remain on the interior pore surfaces after sintering or that partial oxidation of these surfaces has occurred. Future work is required to establish the exact composition of these surfaces.

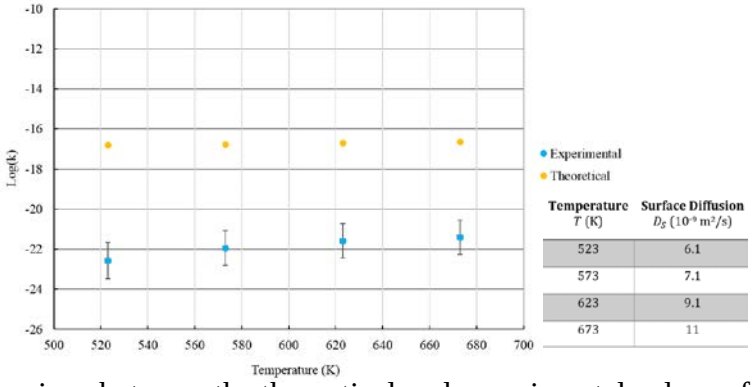

Temperature T (K)	Surface Diffusion D_S (10^{-9} m^2/s)
523	6.1
573	7.1
623	9.1
673	11

Fig. 9. The comparison between the theoretical and experimental values of k, with the values of surface diffusion [29] shown in the accompanying table .

3.2. Observation of microstructural evolution after exposure to air.

One sample from sample set 2 exhibited no change in the exposed exterior surface microstructure after 20 h storage at 300 °C in air. Another sample from this sample set were stored in vacuum and also exhibited no change in exterior microstructure even at 400

°C for 66 h. When the sample stored at 400 °C, indicating no change, was stored for a further 24 h at 500 °C, massive grain coalescence occurred, as seen in Fig. 10. Sample set 3 consisted of samples that were sintered, cross sectioned to expose the interior and then aged at 300 °C. These samples too showed no change in microstructure. Sample set 4 probed whether cleaning of the exterior surface by acid etching would enable microstructural evolution. However, since it was impossible to perform the acid etching in vacuum, the surface was exposed to water and air after etching and no microstructural evolution was observed after storage for 5 h at 300 °C. In summary, the common factor between sample sets 2-4 is that all have been exposed to air, while sample set 1 has not been exposed to air. Lack of microstructural evolution in the exterior is therefore caused by formation of a passivation layer after exposure to the atmosphere. By contrast, the surface under the cover slip underwent rapid evolution, and the changes in microstructure were similar to those observed previously [17-19] when the sintered silver is first aged at 300 °C and then cross sectioned to reveal changes compared to control samples.

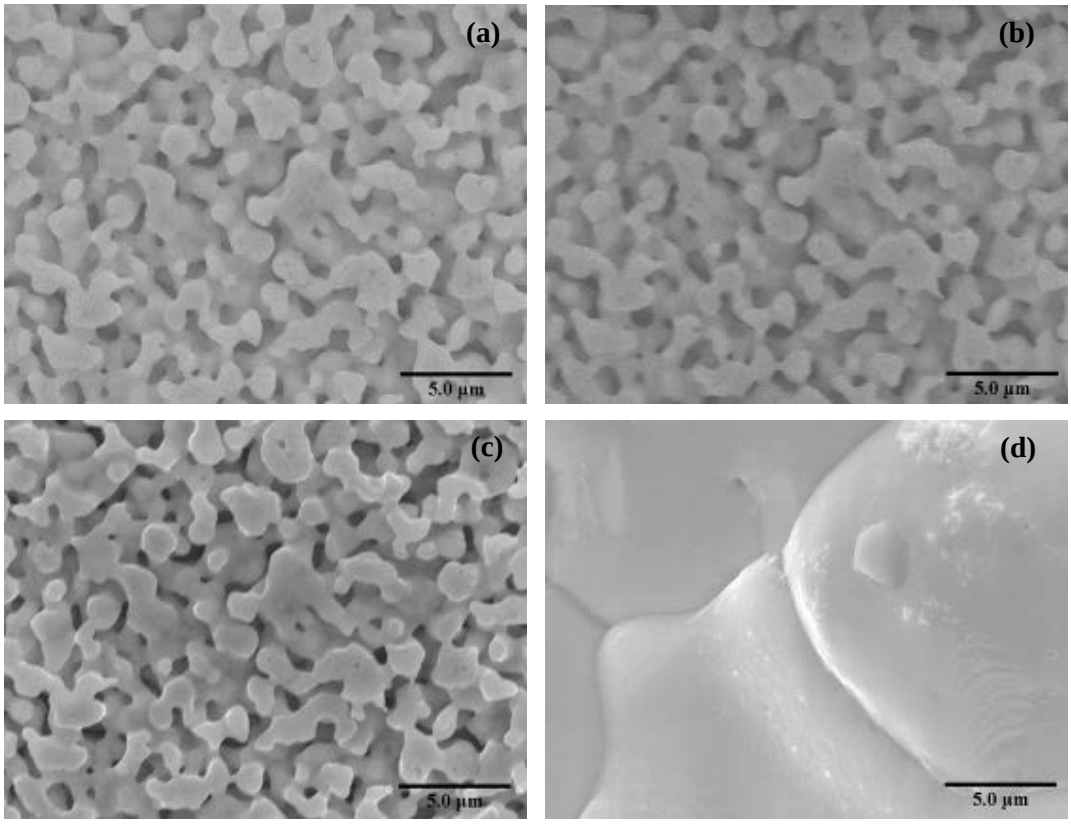

Fig. 10. SEM images of sintered silver from sample set 2. (a) Free surface of sintered silver at 0 h. (b) After storage for 24 h at 300 °C of (a). (c) Additional 16 h at 300 °C and 66 h at 400 °C of area (a) in vacuum. (d) Additional 24 h at 500 °C (not in vacuum, and area (a) could not be identified).

The surface passivation layer blocks atomic surface diffusion, and therefore prevents the changes in grain structure seen in sample set 1 and in the interior of sintered silver in previous work [17-19]. The results indicate that after decomposition of the surface layer at 500 °C, the free movement of silver atoms on the surface of the sample resumed, leading to the morphological changes observed.

Given the change in microstructural behaviour between 400 °C and 500 °C, further investigation of microstructure evolution at 450 °C was carried out on a sample from sample set 2. As can be seen from Fig. 11, 1 h storage of the sample in air did not result in any changes to the morphology of the sample, but after an additional 1.5 h the changes

were significant. During the initial 1 h at 450 °C the surface layer may have decomposed, allowing diffusion and grain evolution to take place during subsequent heating.

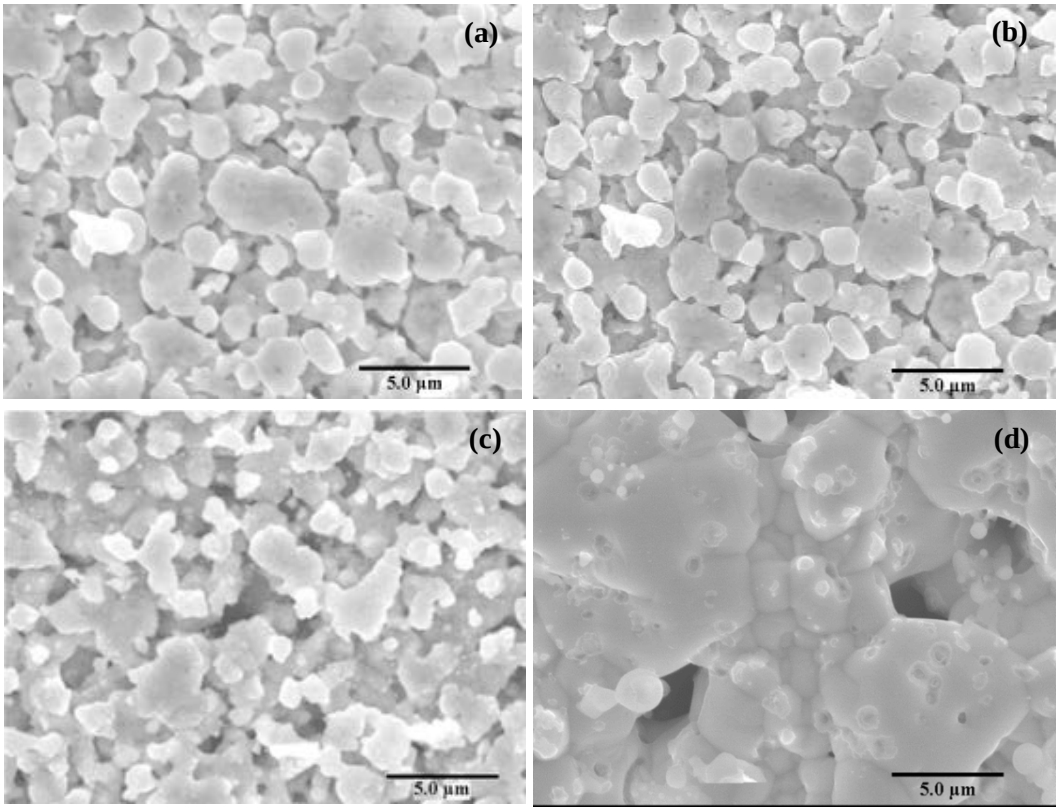

Fig. 11. SEM images of high temperature storage at 450 °C in air. (a) 0 h. (b) 1 h (c) Additional 1.5 h (d) Additional 2.5 h (same area was not identified).

A further test of the presence of a passivating layer on free surfaces (as opposed to surfaces in the interior of the material or protected by glass) was carried out by passing a high current density through samples of sample set 5. Fig. 12 compares the free surface and internal structure of sintered silver before and after 25 days of application of 2.4×10^8 A/cm^2 current density through the material. Fig. 12 (a) and (b) show that on the free surface, electromigration results in the formation of nanorods due to atomic deposition in

the interior of the grains causing stress build-up and eruption of material through the surface passivation layer. However, the overall shapes of the grains have not undergone any other transformation. Fig. 12 (c) and (d) were obtained by cross-sectioning samples before and after electromigration and indicate that in the interior of the material the morphology has radically changed. This shows the presence of a passivating layer on the exposed surfaces of sintered silver preventing the surface diffusion mechanisms, which are active in the interior of the sintered silver material. The temperature in the silver rose only to approximately 100 °C [24] and so electromigration experiments have not proven that the same passivating layer exists in the thermal ageing experiments, since the layer may decompose at the higher temperatures. They do however show that a low temperature passivating layer exists with the same characteristics as those found in the thermal experiments, preventing atomic surface diffusion only at the exterior of the porous material.

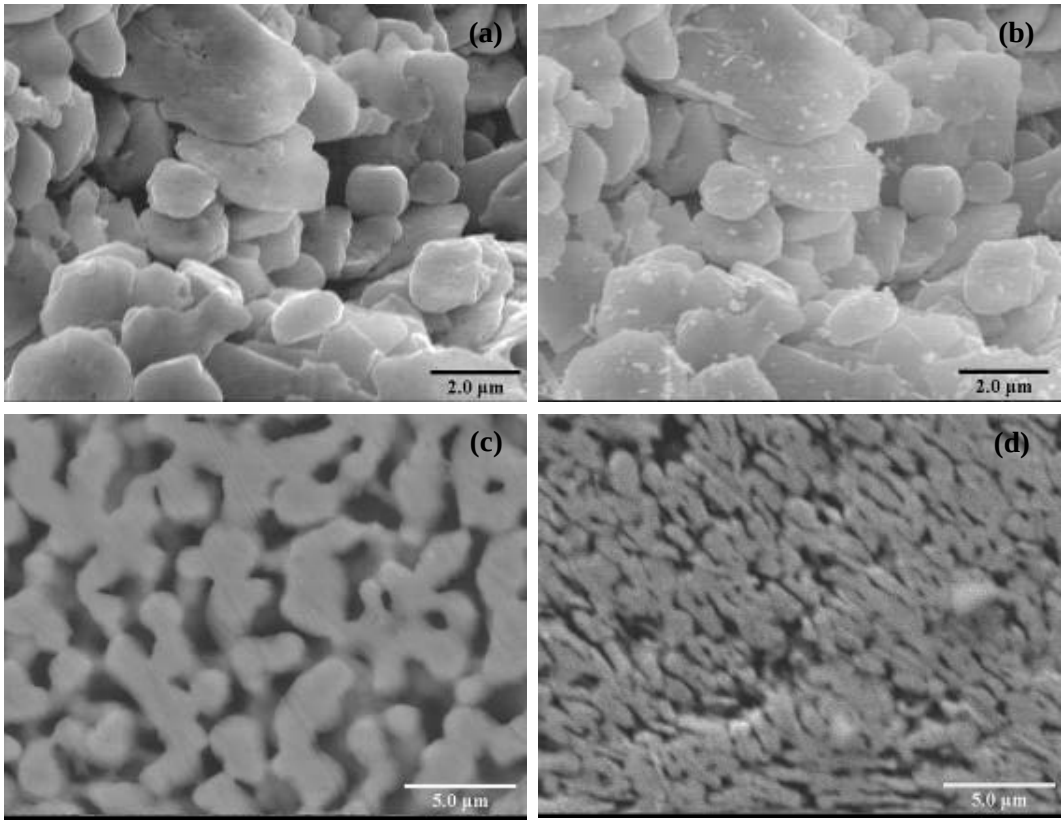

Fig. 12. SEM images for surface and interior evolution comparison. (a) Free surface before passing high current. (b) Free surface after passing high current. (c) Internal structure of a similar sample before passing high current. (d) Internal structure of a sample after passing high current.

Considering the results from sample sets 1-5 as a whole, the passivating layer cannot be due purely to organic compounds from the original paste, as these exist also in the interior of the material, and would have been removed from the exterior by the perchloric acid solution. The presence of oxygen on the free surface of sintered silver has been detected by EDX at room temperature in a similar study [24]. While some studies have shown that some silver oxides start to decompose at 160 °C [30], the second most common type of silver oxide AgO will transform into the most common type Ag_2O at 300 °C [31], and Ag_2O completely decomposes only at 400 °C [32]. Therefore, silver oxide is the most likely composition of the passivating layer.

4. Conclusions

The microstructural behaviour of sintered silver at high temperatures has been investigated both in the absence of exposure to air and after exposure to air. In the absence of exposure to air, while 5 h exposure to 200 °C resulted in no evolution, rapid evolution was observed at temperatures of 250 °C and higher. Therefore, mechanical properties will remain stable, leading to higher reliability assurance for applications up to 200 °C. The grain structure evolution has been mapped out for different temperatures and it has been found that evolution consists of rapid growth stages interspersed with periods of relative stability. This evolution was studied in detail, tracking individual pores and grains. The activation energy of grain growth for the silver grains has been calculated as 52.5 (±2.5) KJ/mol, which agrees with the literature value. However, exposure to atmosphere of the sintered silver surface stops the surface diffusion of silver atoms and preserves the initial microstructure. This phenomenon results in a stable structure on the free surface of sintered silver even at 400 °C. The stabilizing passivation layer is most likely to be silver oxide. The presence of the passivation layer was independently confirmed using a novel electromigration based technique which probed surface diffusivity of atoms in the interior of the sample. Moreover, the studies on the mechanical properties of sintered silver associate the coarsening of the grain structure with deterioration of mechanical properties [7, 9, 17-19, 33, 34], so that if the passivation layer could be grown in the interior of the material at the last stage of the sintering process, utilizing temperature triggered oxidation agents in the paste, then joint lifetimes could potentially be increased. The final conclusion is that until methods for stabilizing the microstructure above 200 °C are found, extensive long-term testing of mechanical properties during storage is required to ensure that joints

formed from sintered silver retain adequate strength. Alternative solutions do also exist, but require the addition of interposers along with the sintered silver to produce a thermally stable die attach, increasing the high temperature reliability [35].

Acknowledgements

The authors would like to thank Messrs. Geoff Lewis and Graham Dumas from Eltek Semiconductors Ltd for supply of materials and Messrs Ernest Samuel and William Luckhurst for their help during the experimental procedures.

References

[1] V. R. Manikam, K. Y. Cheong, Die Attach Materials for High Temperature Applications: A Review, IEEE Trans. Compon. Packag. Manuf. Technol. 4 (2011) 457–478.

[2] T. A. Tollefsen, O. M. Løvvik, K. Aasmundtveit, A. Larsson, Effect of temperature on the die shear strength of a Au–Sn SLID bond, Metall. Mater. Trans. A 44(7) (2013) 2914–2916.

[3] H. Li, P. D. Han, X. B. Zhang, M. Li, Size-dependent melting point of nanoparticles based on bond number calculation, Mater. Chem. Phys. 137 (2013) 1007-1011.

[4] M. Maruyama, R. Matsubayashi, H. Iwakuro, S. Isoda, T. Komatsu, Silver nanosintering: a lead-free alternative to soldering, Appl. Phys. A 93 (2008) 467-470.

[5] Y. Akada, H. Tatsumi, T. Yamaguchi, A. Hirose, T. Morita, E. Ide, Interfacial bonding mechanism using silver metallo-organic nanoparticles to bulk metals and observation of sintering behavior, Mater. Trans. 49 (2008) 1537-1545.

[6] J.G. Bai, G. Q. Lu, ⊤hermomechanical reliability of low-temperature sintered silver die attached SiC power device assembly, IEEE Trans. Device Mater. Reliab. 6 (2006) 436-441.

[7] V. Caccuri, X. Milhet, P. Gadaud, D. Bertheau, M. Gerland, Mechanical Properties of Sintered Ag as a New Material for Die Bonding: Influence of the Density, J. Electron. Mater. 43 (2014) 4510-4514.

[8] K.S. Siow, Mechanical properties of nano-silver joints as die attach materials, J. Alloys Compd. 514 (2012) 6-19.

[9] K. S. Siow, Are Sintered Silver Joints Ready for Use as Interconnect Material in Microelectronic Packaging?, J. Electron. Mater. 1 (2014) 947-961.

[10] K. Nakaso, M. Shimada, K. Okuyama, K. Deppert, Evaluation of the change in the morphology of gold nanoparticles during sintering, J. Aerosol Sci. 33 (2002) 1061-1074.

[11] A. Moitra, S. Kim, S.-G. Kim, S.J. Park, R.M. German, M.F. Horstemeyer, Investigation on sintering mechanism of nanoscale tungsten powder based on atomistic simulation, Acta Mater. 58 (2010) 3939-3951.

[12] E. Ide, S. Angata, A. Hirose, K.F. Kobayashi, Metal–metal bonding process using Ag metallo-organic nanoparticles, Acta Mater. 53 (2005) 2385-2393.

[13] P. Peng, A. Hu, B. Zhao, A.P. Gerlich, Y.N. Zhou, Reinforcement of Ag nanoparticle paste with nanowires for low temperature pressureless bonding, J. Mater. Sci. 47 (2012) 6801-6811.

[14] M. Puchalski, P. J. Kowalczyk, I. Zasada, P. Krukowski, W. Olejniczak, Alloying process at the interface of silver nanoparticles deposited on Au (111) substrate due to the high-temperature treatments. J. Alloys Compd. 481(1) (2009) 486-491.

[15] M. Edwards, K. Brinkfeldt, U. Rusche, T. Bukes, G. Gaiser, M. Da Silva, and D. Andersson, The shear strength of nano-Ag sintered joints and the use of Ag interconnects in the design and manufacture of SiGe-based thermo-electric modules. Microelectron. Reliab. 55(5) (2015) 722-732.

[16] L. C. Wai, W. W. Seit, E. P. J. Rong, M. Z. Ding, V. S. Rao, D. R. MinWoo, Study on silver sintered die attach material with different metal surfaces for high temperature and high pressure (300° c/30kpsi) applications. Electronics Packaging Technology Conference 2013 (EPTC 2013), IEEE Singapore, (2013) 335-340.

[17] G. Dumas, G. Lewis, S. H. Mannan, Evaluation of pressure free nanoparticle sintered silver die attach on silver and gold surfaces, HiTEN 2013, IMAPS Oxford, (2013) 237 – 245.

[18] F. Yu, R.W. Johnson, M. Hamilton, Low Temperature, Fast Sintering of Micro-Scale Silver Paste for Die Attach for 300° C Applications, HiTEC 2014, IMAPS, Albuquerque, (2014) 654-660.

[19] S. Paknejad, G. Dumas, G. West, G. Lewis, S. Mannan, Microstructure evolution during 300 °C storage of sintered Ag nanoparticles on Ag and Au substrates, J. Alloys Compd. 617 (2014) 994-1001.

[20] S. A. Paknejad, A. Mansourian, Y. Noh, K. Khtatba, L. Van Parijs, S. H. Mannan, Factors influencing microstructural evolution in nanoparticle sintered Ag die attach, HiTEN 2015, IMAPS Cambridge, (2015) 50-58.

[21] B. Shoelson, ThresholdLocally. Accessed on 13/04/2015 from http://www.mathworks.com/matlabcentral/fileexchange/29764-thresholdlocally, last update 08/02/2011.

[22] D. L. Van Hyning, C. F. Zukoski. Formation mechanisms and aggregation behavior of borohydride reduced silver particles. Langmuir *14*(24) (1998) 7034-7046.

[23] D. N. Craig, C. A. Law, W. J. Hamer. Stability of silver and Pyrex in perchloric acid-silver perchlorate solutions and in conductivity water. J. Res. Nat. Bur. Stand. (1960) 127-34.

[24] A. Mansourian, S. A. Paknejad, Q Wen, G. Vizcay-Barrena, R. A. Fleck, A. V. Zayats, S. H. Mannan, Tunable Ultra-high Aspect Ratio Nanorod Architectures grown on Porous Substrate via Electromigration, Sci. Rep. 6 (2016) 22272.

[25] Z. Fang, H. Wang, Densification and grain growth during sintering of nanosized particles, Int. Mater. Rev. 53 (2008) 326-352.

[26] R. Dannenberg, E. Stach, J.R. Groza, B.J. Dresser, TEM annealing study of normal grain growth in silver thin films, Thin Solid Films, 379 (2000) 133-138.

[27] Y. Nishida. Introduction to Metal Matrix Composites: Fabrication and Recycling, Springer Sci. & Bus. Media (2013).

[28] R. Castro, K. van Benthem (Eds.). Sintering: mechanisms of convention nanodensification and field assisted processes. Vol. 35, Springer Sci. & Bus. Media 35 (2012) 11-12.

[29] G. Antczak, G. Ehrlich. Surface diffusion: metals, metal atoms, and clusters. Cambridge Univ. Press (2010).

[30] J. Tominaga, The application of silver oxide thin films to plasmon photonic devices. J. Phys.: Condens. Matter 15(25) (2003) R1101.

[31] G. B. Hoflund, Z. F. Hazos, G. N. Salaita, Surface characterization study of Ag, AgO, and Ag 2 O using X-ray photoelectron spectroscopy and electron energy-loss spectroscopy. Phys. Rev. B 62(16) (2000) 11126-11133.

[32] T. Morita, Y. Yasuda, E. Ide, Y. Akada, A. Hirose, Bonding technique using micro-scaled silver-oxide particles for in-situ formation of silver nanoparticles, Mater. Trans. 49 (2008) 2875-2880.

[33] X. Milhet, P. Gadaud, V. Caccuri, D. Bertheau, D. Mellier, M. Gerland, Influence of the Porous Microstructure on the Elastic Properties of Sintered Ag Paste as Replacement Material for Die Attachment. J. Electron. Mater. 44(10) (2015) 3948-3956.

[34] J. Carr, X. Milhet, P. Gadaud, S. A. Boyer, G. E. Thompson, P. Lee, Quantitative characterization of porosity and determination of elastic modulus for sintered micro-silver joints. J. Mater. Process. Technol. 225 (2015) 19-23.

[35] S. A. Paknejad, A. Mansourian, Y. Noh, K. Khtatba, S. H. Mannan, Thermally stable high temperature die attach solution, Mater. Des. 89 (2015) 1310-1314.